International Journal of Science and Research (IJSR)
ISSN (Online): 2319-7064
Index Copernicus Value (2013): 6.14 | Impact Factor (2013): 4.438

Diagnosis and Classification of Liver Cancer using LIBS Technique and Artificial Neural Network

Ashraf M. EL Sherbini[1], Mohamed M. Hagras[2], Hania H. Farag[2], Mohamed R.M. Rizk[2]

[1]Laboratory of Lasers and New Materials (LLNM), Faculty of Science, Cairo Univ., Egypt

[2]Faculty of Engineering, University of Alexandria, Egypt

Abstract: ***(LIBS) technique was used to diagnose liver cancer. Radiation from Nd: YAG laser at 532 nm with 5.7x10^8 W/cm^2 was used to initiate plasma on surface of liver tissue. The light emitted was analyzed which allowed detection of trace elements in malignant tissue. Twenty six malignant samples in the age range from 6 to 56 years were categorized into 4 sets with different levels of malignancy depending on histological analysis. The following trace elements Mg, K, Ca, Na, Fe, Mn and Cu were identify. The concentration of the different trace elements was found to steeply rise with category #1 in the malignant tissues in comparison to the normal (Zero) ones by a factors of x 6.5, 2.5, 7, 4.5, 7, 6.5, 2.5, respectively with a further increase as we pass from category #2 to #4, with much slower rates. The results from the LIBS-Technique were fed-back to an artificial neural network (ANN) to take a decision about the classification of the cancer. A confirmation of about 80 % was found in close agreement with standard documented international values.***

Keywords: LIBS, Liver Cancer, ANN, OES.

1. Introduction

LIBS-is an acronym standing for "Laser Induced Breakdown Spectroscopy". The technique is based on analyzing light emitted from plasma generated by interaction of a high power lasers with matter (solid, liquid or gases). Assuming that light emitted is sufficiently influenced by the characteristic parameters of the plasma, the analysis of this light clears considerable information about the elemental structure and concentration in the irradiated samples [1]. The LIBS-technique becomes one of the most applied chemical analytical techniques because of its inherent well known advantages e.g. reliability, minimal destructive, non-contact optical nature, freedom from sample preparation [2] and acceptable limit of detection [3]. The biomedical applications of LIBS can be broadly classified into two categories [4]; first is the analysis of human clinical specimens (which may be teeth, bones, tissue samples, blood or other fluid samples) [5] and second the analysis of microorganisms (e.g. bacteria, moulds, yeasts) that can infect human objects and cause disease [6].

LIBS-technique was recognized very early as a potentially useful tool for the analysis of calcified tissues such as teeth [7]. Samek et al [7] had performed quantitative LIBS analysis of trace element concentration in calcified tissue. Fang et al. [8] used LIBS to analyze and identify elemental constituents of urinary calculi. Yueh [9] performed LIBS on tissue specimens from the brain, lung, spleen, liver, kidney and skeletal muscle and determined that LIBS can discriminate between different tissue types. Recent studies on the changes in the level of some elements such as Ca, Fe, and Mn was done with malignant cells can be found in Ref. [10]. Imam et.al used LIBS technique and showed that there is an increase in the concentration levels of the elements (Ca, Zn, Cu, Mn, and Fe) in the malignant breast tissue compared with the normal ones [11]. EL Hussein et al (2010) were able to diagnose some types of human malignancies. Cancerous tissues could be distinguished from non-cancerous tissues by looking at calcium and magnesium amounts [12].

LIBS has already been used to effectively distinguish normal and malignant tumor cells from histological sections and to characterize several types of human malignancies [13], to determine the trace metal concentrations in human hair and skin samples [14, 15], to determine the elemental composition of liver, kidney, muscle, and hepatopancreas tissues [16] and even to perform screening of whole human blood [17]. Kumar et al [18, 19] demonstrated in principle that LIBS can be used for tissue analysis, specially the ability to differentiate between malignant and normal tissue.

On the other hand, Inakollu [20] used the artificial neural network ANN to predict the element concentrations in aluminum alloys from its LIBS spectrum. Ferreira [21] selected a set of wavelengths through the "wrapper" algorithm and then determined the concentration of copper in soil samples by ANN. Sattmann [22] discriminated PVC from other polymers with the distinct chlorine 725.66 nm line. Ramil et al [23] classified the LIBS spectra of 36 archaeological ceramics into three groups by ANN. The possibility of using ANN to predict composition in natural rocks was explored in earlier works by Motto-Ros et al [24] and Koujelev et al [25]. The capability of mineral and rock sample identification with LIBS combined with ANN was also demonstrated in [25]. The potential of ANN to analyze LIBS spectra has been proven in these studies.

In this work and for the first time, we report the change of the level of (Mg, K, Ca, Na, Fe, Mn and Cu) in liver tissue which is the trace elements in the liver tissue by LIBS. An increase in the elemental concentrations of the elements was found and can be attributed to the cancer formation in liver. Feeding the results obtained from the (LIBS) technique into a neural network enabled us to take a decision about the classification of the tissue whether normal or malignant.

2. Experimental LIBS-setup

Figure 1, depicts the basic set up, the experiment is performed in such a way that a Q-Switched Nd: YAG laser (type Brilliant B from Quantel) was used for inducing plasma from samples surface in open air. The Nd: YAG laser was operated at wavelength 532 nm, with energy per pulse of ~ 125 mJ was measured at the target surface using a power meter (Ophier, model 1z02165). The pulse duration was 5 ns and overall irradiance of ~ 5.7 $x10^8$ W/cm^2. The reflection from the beam splitter was measured and found to be ~ 6% while the absorption through it was found to be ~ 6.6 % of the laser energy. The optical fiber used is multimode quartz with a 25 µm inner diameter and was mounted on xyz-translational stage, which enabled us to align it with the centerline of the plume to ensure that the emission signal was collected perpendicularly with respect to its symmetry axes. The optical fiber was connected to an echelle type spectrograph (model SE200 from Catalina®) via SMA connector.

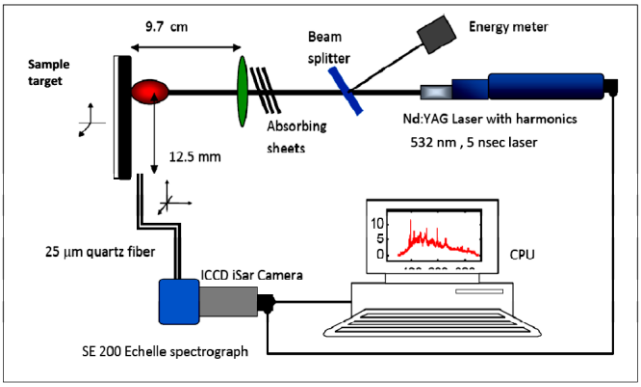

Figure 1: A schematic diagram of experimental set up

The spectrograph is coupled to an intensified charge coupled device (ICCD) camera (type Andor, model iStar DH734-18F). The entrance aperture of a spectrograph is a circular opening 25 µm in diameter, and the ICCD is contained in a camera head mounted at the exit port. Light emission is collected by scanning the ICCD over the wavelengths of interest. The system was controlled by Kestrel-Spec® software to acquire images from the supported camera. The system of detection covered a wavelength range from 200 to 1000 nm in single shot. The spectral intensity of the lines is recorded as a fixed delay and date times of 1 µs. The identification of the different elements was carried using span16 software spectrum analyzer®. The analysis and manipulation of the data was carried using a special homemade software routine built under MATLAB® package. The wavelength axis was calibrated using light from a low pressure Hg- lamp (Ocean optics HG-1). A Deuterium-Halogen lamp (type Ocean optics, model Dh-2000-CAL), was used in calibrating the emission spectral intensities (relative sensitivity) over the entire wavelength scale.

3. Materials and Method

Twenty six samples were selected from patients in the ages between 6 to 56 years, as well as 4 normal (zero cancer level). Each of these samples was doubled so as to allow for pathological analysis to be made in parallel to the LIBS-analysis to avoid any interference in the LIBS spectra arises from the digestion methodologies used in histological analysis. Pathological analysis shows that, sixteen surgical specimens were obtained by decisional biopsy and fourteen by radical operation. All specimens were fixed in formalin (10% formaldehyde in water) and then histologically processed to form paraffin blocks, which were sectioned at 4 µm thickness using a microtome. These sections were layered on a glass slide for staining and the slides were embedded for 2 minutes in hematoxylin (which stains the nuclei blue) and then eosin (which stains the cytoplasm and the extracellular connective tissue matrix pink). The histological slides were finally examined under a microscope (type Olympus CX_{31}). The samples were then digested using a simple efficient digestion method dry weight technique. For a rapid sample preparation and quantification, assisted acid digestion by concentrated nitric acid method was used. After digestion the samples were diluted using distilled water.

4. Results and Discussion

The identified fingerprint spectral lines are collected and presented in Table 1. One should notice that, the existence of the hydrogen is indicated by the existence of the $H_{\square}$-line at 656.3 nm, while the oxygen by two lines at 777.19 and 844.63 nm lines and nitrogen by six lines as indicated in Table 1.

However, the suspected elements (Iron, manganese sodium and magnesium) are confirmed by large number of the fingerprint lines as given in table 1; whereas the existence of the copper is confirmed by one line at 570.02 nm line. In quantitative analysis one should be careful about the spectrograph and camera relative sensitivity. This is because the ICCD camera pixels are not equally sensitive to all the recorded wavelengths. Therefore, we have calibrated the experimental setup using the lamp (Dh-2000 CAL). The results of the recorded emission from plasmas initiated from the surface of category #1 in comparison to zero cancer (normal) category level are shown in Figures. 2 a-h. In these figures one can see an increase in the spectral radiance of the different elements existing in both samples. From this figure the amount of enhanced emission is different for identified elements which indicate different rates of increase of trace elements, as observed by several authors [11-14] and listed in Table 1. From the statistical point of view, in order to calculate the contribution of each identified element, one has to take the average of spectral radiances over the emitted wavelengths from certain element and then fed to histogram plot.

Table 1: A list of the identified elements utilizing LIBS – from liver tissue

Identified element	Sym.	Z	Wavelength (nm)
1. Hydrogen	H	1	656.27
2. Oxygen	O	8	777.19, 844.63
3. Nitrogen	N	7	868.34, 865.58 , 862.92 , 746.83, 744.26, 742.36
4. Copper	Cu	29	570.02
5. Magnesium	Mg	12	383.23, 383.82
6. Potassium	K	19	850.34, 766.49
7. Sodium	Na	11	819.94, 818.32, 589.59 ,588.99
8. Calcium	Ca	20	422.67, 428.93, 430.25, 430.77, 445.58, 526.55, 527.02, 610.27 ,612.22, 616.37,
9. Manganese	Mn	25	279.48, 280.10, ,317.85
10. Iron	Fe	26	252.47, 263.22, 370.78, 373.71, 385.63, 390.64, 393.02, 396.92, 428.24, 431.50, 517.15

Figure 3; shows the histogram of the average spectral radiance from different elements arises from different 4 categories with respect to zero level cancer specimens in terms of their respective atomic number. One can notice the strong increase of the height (i.e. the relative concentration) of the same elements present in the infected tissue of category #1 with respect to the zero level tissue, as well the emission from gaseous elements e.g. nitrogen and oxygen. Moreover, from Figure 4, one can deduce that, the increase in the relative concentration was found rather weak as we pass from category #2 up to #4, which means that, the cancer starts to work even if the concentration of the different identified trace elements (Mg, K, Ca, Na, Fe, Mn and Cu) is infinitesimally increased.

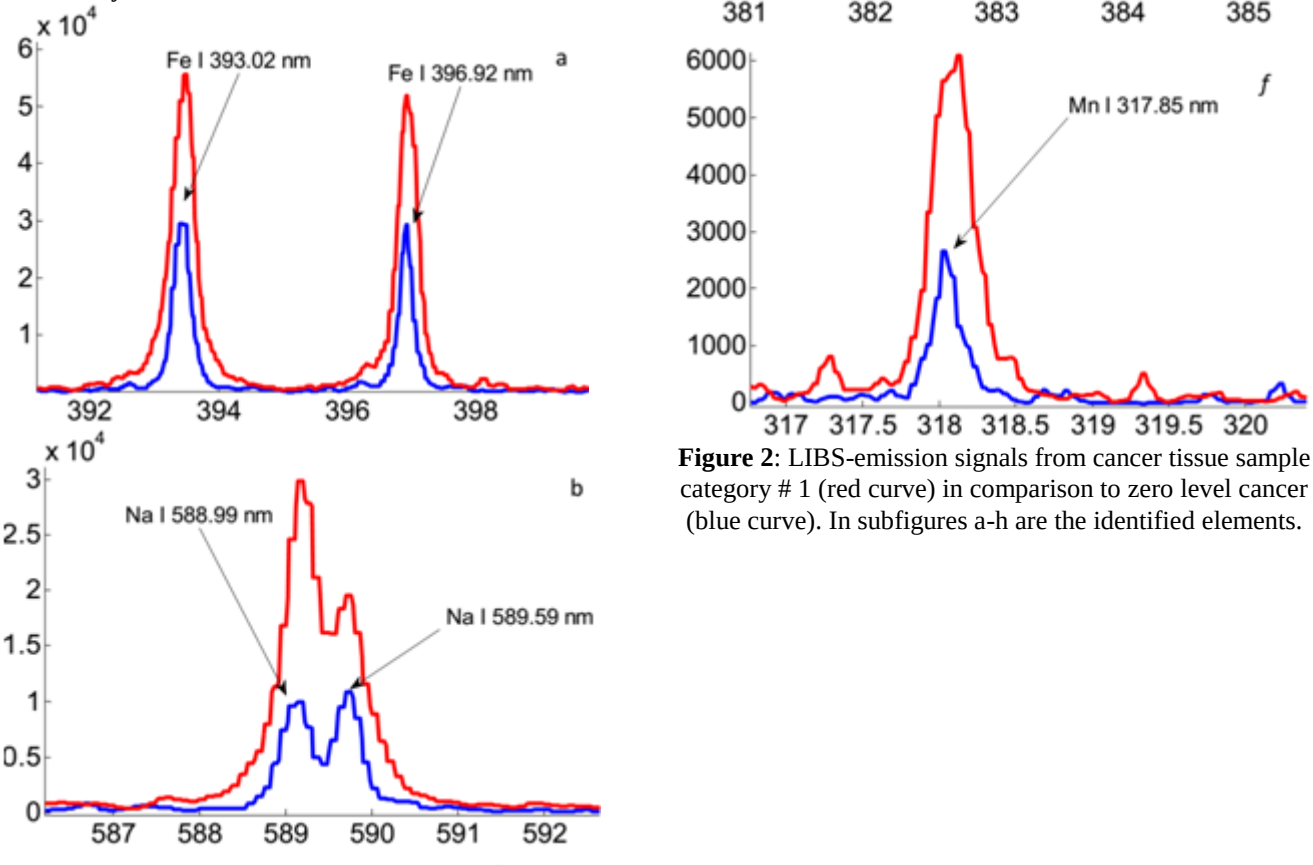

Figure 2: LIBS-emission signals from cancer tissue sample category # 1 (red curve) in comparison to zero level cancer (blue curve). In subfigures a-h are the identified elements.

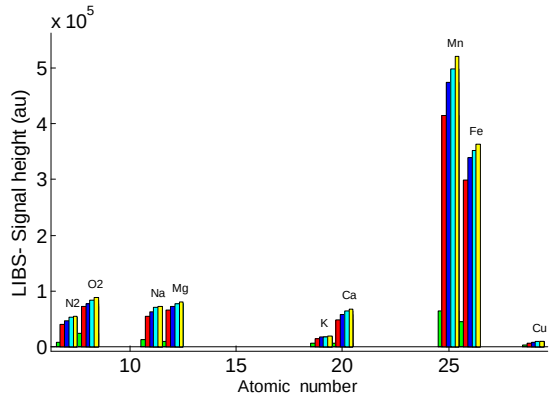

Figure 3: Histogram distribution of the average of LIBS signals from different elements with atomic number, Green is the zero level cancer; red is category #1; blue is category #2; cyan category #3and yellow category #4.

In order to determine precisely which element increases more than others and may be responsible the liver cancer, one has to reconstruct another histogram showing the rate of increase of different trace element concentrations which is shown in Figure 5. This figure undoubtedly clears the relation between elemental concentration of certain elements and the malignant liver tissue

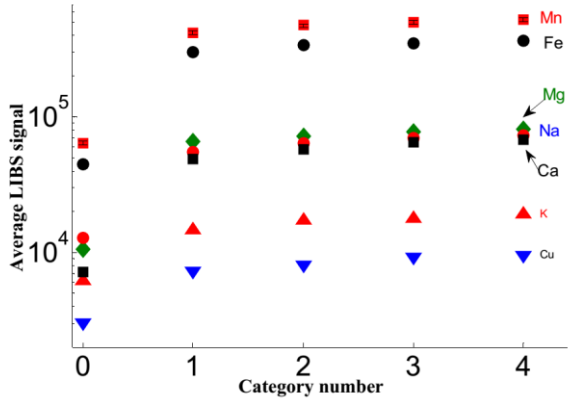

Figure 4: The variation of the average LIBS signal from different elements identified with different categories.

.

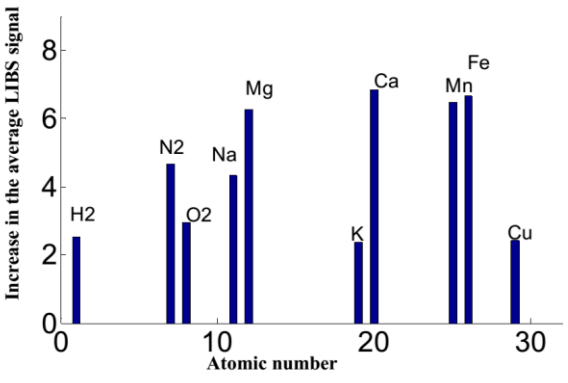

Figure 5: Demonstration of the increase in the LIBS signals (relative concentration) arises from different elements from the zero level samples (normal) with respect to that from category #1.

Finally we constructed a pattern recognition neural network as shown in Figure 6a. The training algorithm is scaled conjugate gradient back propagation .The performance of ANN 84.1% as indicated in Figure 6b. The best validation performance of the neural network is shown in Figure 7. It can differentiate between normal and malignant samples. The decision of the neural network for all 30 samples is given in Table 2. The neural network can recognize all the malignant samples and the normal samples for all 30 samples correctly except sample no. 9.

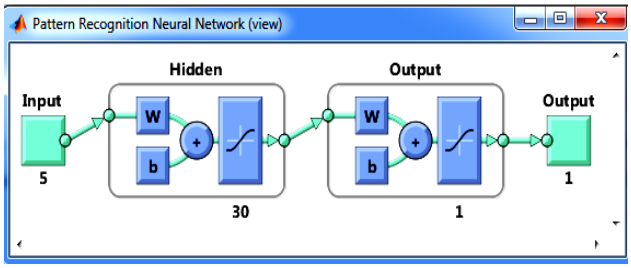

Figure 6a: the constructed NN

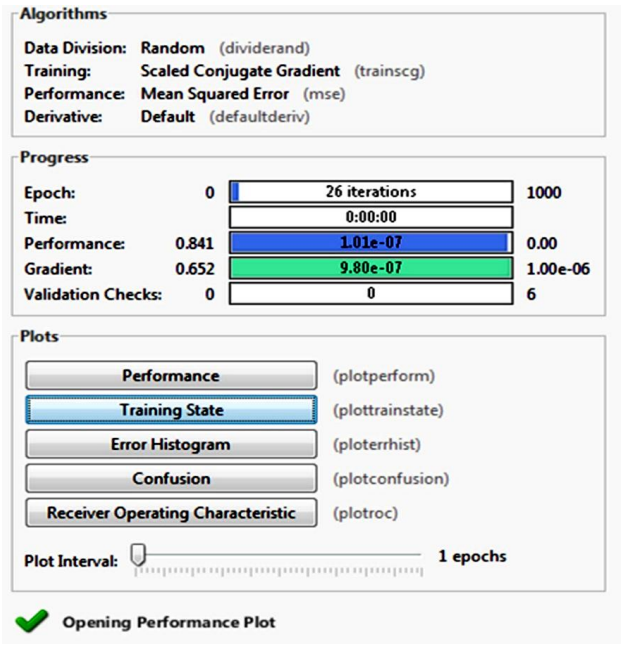

Figure 6b: Shown is the progress of our ANN

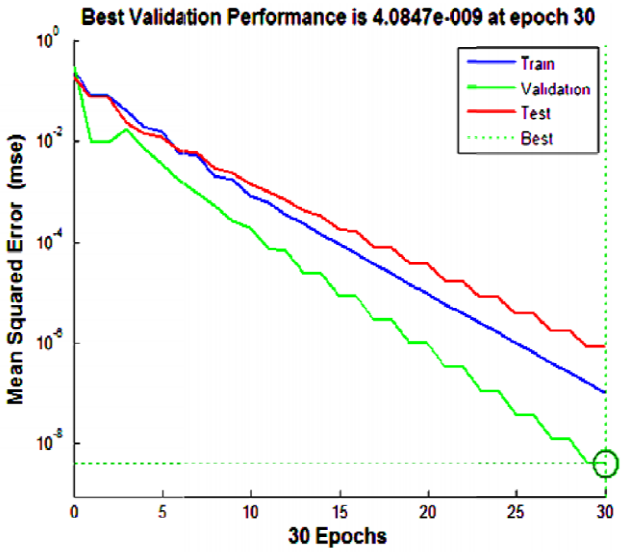

Figure 7: The performance curve of the neural network

Table 2: Decision factor using the voting algorithm

Ser	Mg	Na	Ca	Mn	Fe	State	D
1	10506	12780	7203	64007	44920	N	0
2	19506	10780	92039	94007	64920	N	0
3	16516	12138	10899	90950	62886	N	0
4	19924	12739	11777	1.28e5	61191	N	0
5	9310	34147	28916	289160	232710	G1	1
6	62082	61649	56553	3.87e5	2.82e5	G1	1
7	73570	72141	63309	5.16e5	4.06e5	G1	1
8	70439	51556	45367	4.85e5	2.79e5	G1	1
9	77206	59455	52594	4.79e5	3.31e5	G1	0
10	70454	66913	58994	5.29e5	3.68e5	G1	1
11	61597	48286	42263	3.30e5	2.36e5	G1	1
12	78116	58328	52637	4.57e5	3.52e5	G1	1
13	49035	41056	38143	2.57e5	2.04e5	G1	1
14	70183	54355	51343	3.18e5	2.47e5	G2	1
15	77210	59294	52821	4.92e5	3.21e5	G2	1
16	73261	68905	63027	4.30e5	3.50e5	G2	1
17	89603	75524	68001	4.69e5	4.37e5	G2	1
18	72718	68524	62319	4.73e5	3.42e5	G2	1
19	57437	44722	39565	3.84e5	2.71e5	G2	1
20	69803	84739	75929	80270	3.39e5	G2	1
21	70408	61886	55135	5.36e5	3.52e5	G2	1
22	69657	55986	50011	4.78e5	3.00e5	G2	1
23	80232	76735	71598	4.89e5	3.42e5	G3	1
24	83682	64701	56798	5.48e5	3.37e5	G3	1
25	82561	58069	54348	4.14e5	3.11e5	G3	1
26	71176	69260	61528	584660	372260	G3	1
27	80655	73768	67725	523170	342740	G3	1
28	62515	52708	48895	382620	353590	G3	1
29	80368	58964	52324	449340	334250	G3	1
30	80434	110070	104790	594660	415530	G3	1

5. Conclusions

The elements (Mg, K, Ca, Na, Fe, Mn and Cu) in the human liver were identified in a simple manner using LIBS-Technique. The presented findings suggest an association of the increase in elemental compositions of (Mg, K, Ca, Na, Fe, Mn and Cu), by a factors of X6.5, 2.5, 7, 4.5, 7, 6.5, 2.5 in liver tissues and liver cancer. In other words, the increase in the elemental concentrations and clustered calcifications in the liver maybe related. And finally the results show that using the ANN is useful to classify the liver tissues to be whether normal or malignant. Specifically, we can draw the following four conclusions about the LIBS-Technique as:

- Simple and promising technique is capable of diagnosing malignant cells and tissues.
- It reduces the possibility of contamination as well as standard errors.
- Is minimally invasive, since a small-sized sample can generate good results.
- Gives online quantification for all trace elements in a tissue simultaneously.

Future work should include enhancing the voting algorithm in order to assess the degrees of deviation of malignant cells from normal cells and thus deduce the cancer grade The enhancing mechanism could also include the study of building combined techniques that use more complex algorithms that could avail the advantage of LIBS results.

6. Acknowledgement

The experimental part and theoretical analysis were carried out at the Lab. of Lasers and New Materials (LLNM), Phys. Dep., Cairo University. The authors would to thank Prof. Th. M. EL Sherbini for allow to use the experimental facilities.

References

[1] F. Yueh, J. P. Singh, and H. Zhang "Laser-induced Breakdown Spectroscopy", Elemental Analysis, Encyclopaedia of Analytical Chemistry, R.A. Meyers (Ed.), John Wiley & Sons Ltd, Chichester, 2066-2087 (2000).

[2] X. Fang and S. R. Ahmad, "Elemental analysis in environmental and samples by stand-off laser-induced breakdown spectroscopy", Appl. Physics B, 115, 4, pp 497-503, (2014).

[3] W. T. Y Mohamed et al "Improved LIBS limit of detection of Be, Mg, Si, Mn, Fe and Cu in aluminum alloy samples using a portable Echelle spectrometer with ICCD camera", Optics & Laser Technology, 40, 1, pp 30–38, (2008).

[4] V. K. Singh, V.Kumar, J. Sharma, Y. Khajuria, and K. Kumar, "Importance of Laser Induced Breakdown Spectroscopy for Biomedical Applications: A Comprehensive Review", 3, 3, pp. 169-182, (2014).

[5] S. J. Rehse, H. Salimnia, and A. W. Miziolek, "Laser-induced breakdown spectroscopy (LIBS): an overview of recent progress and future potential for biomedical applications", J. Med. Eng. Technol., 36, 2, pp.77-89, (2012).

[6] S. Morel, N. Leone, P. Adam, and J. Amouroux, "Detection of bacteria by time-resolved laser-induced breakdown spectroscopy", Applied Optics, 42, 30, pp. 6184-6191, (2003).

[7] O. Samek, H. H. Telle and D. C. S. Beddows, "Laser-induced breakdown spectroscopy: a tool for real-time, in vitro and in vivo identification of carious teeth", BMC Oral Health, 1, PMC64785, ISSN: 14726831, (2001).

[8] X. Fang, S. R. Ahmad, M. Mayo and S. Iqbal " Elemental analysis of urinary calculi by laser induced plasma spectroscopy", Lasers in Medical Science, 20, 132,(2005).

[9] F.Y. Yueh, H. Zheng, J. P. Singh and S. Burgess, "Preliminary evaluation of laser-induced breakdown spectroscopy for tissue classification", Spectrochim. Acta Part B: 64, 10, pp.1059 -1067, (2009).

[10] J. G. Liehr and J. S. Jones, "Role of iron in estrogen-induced cancer", Curr Med Chem .8, pp.839–849, (2001).

[11] H. Imam, R. Mohamed and A. A. Eldakrouri, "Primary Study of the Use of Laser-Induced Plasma Spectroscopy for the Diagnosis of Breast Cancer", Opt. and Phot. J, 2, pp.193-199, (2012).

[12] A. El-Hussein, A. K. Kassem, H. Ismail and M. A. Harith "Exploiting LIBS as a spectrochemical analytical technique in diagnosis of some types of human malignancies", Talanta, 82, pp.495–501, (2010).

[13] J. Kaiser, K. Novotny, M. Z. Martin, A. Hrdlicka, R. Malina, M. Hartl, V. Adam and R. Kizek "Trace elemental analysis by laser-induced breakdown

spectroscopy—Biological applications", Surface Science Reports, 67, pp. 233–243, (2012).
[14] X-Y. Liu, W-J Zhang, "Recent developments in biomedicine fields for laser induced breakdown spectroscopy", J. Biomedical Science and Engineering, 1, pp.147-151, (2008).
[15] B. Vinod, and P. P. Haroled, "Laser Induced Breakdown Spectroscopy: A Novel Technique in Research", International Journal of Research in Pharmaceutical and Biomedical Sciences, 3, 3, pp.1360-1370, (2012).
[16] D. Jr. Santos, R. E. Samad, L. C. Trevizan, A. Z. De Freitas, N. D. Jr. Vieira And F. J. Krug " Evaluation of Femtosecond Laser-Induced Breakdown Spectroscopy for Analysis of Animal Tissues", Appl. Spectroscopy, 62, 10, pp.1137-1143, (2008).
[17] N. Melikechi, H. Ding, S. Rock, O. Marcano and D. Connolly, "Laser-induced breakdown spectroscopy of whole blood and other liquid organic compounds", Proceedings SPIE, 6863, pp.1–7, (2008).
[18] A. Kumar, F-Y. J. Yueh, P. Singh and S. Burgess, "Characterization of malignant tissue cells by laser-induced breakdown spectroscopy", Appl. Opt. 43, No.28, pp.5399-5401, (2004).
[19] D. E. Lewis, J. Martinez, C.A. Akpovo, L. Johnson, A. Chauhan and M.D. Edington "Discrimination of bacteria from Jamaican bauxite soils using laser-induced breakdown spectroscopy. 401, 7, pp2225-2236, (2011).
[20] P. Inakollu, T. Philip, A. K. Rai, F.-Y. Yueh, and J.P. Singh, "A comparative study of laser induced breakdown spectroscopy analysis for element concentrations in aluminum alloy using artificial neural networks and calibration methods", Spectrochim. Acta Part B, 64, 1, pp. 99-104,(2009).
[21] E. C. Ferreira, D. M. B. P. Milori, E. J. Ferreira, R. M. Da Silva and L. Martin-Neto "Artificial neural network for Cu quantitative determination in soil using a portable laser induced breakdown spectroscopy system", Spectrochim. Acta Part B, 63, 10, pp. 1216-1220, (2008).
[22] R. Sattmann, I. Mönch, H. Krause, R. Noll, S. Couris, A. Hatziapostolou, A. Mavromanolakis, C. Fotakis, E. Larrauri and R. Miguel "Laser-induced breakdown spectroscopy for polymer identification", Appl. Spect., 52, 3, pp. 456-461, (1998).
[23] A. Ramil, A.J. López, and A. Yáñez "Application of artificial neural networks for therapid classification of archaeological ceramics by means of laser induced breakdown spectroscopy (LIBS)", Appl. Phys, A, 92, 1, pp. 197-202, (2008).
[24] V. Motto-Ros, A. S. Koujelev, G. R. Osinski, and A.E. Dudelzak "Quantitative multielemental laser-induced breakdown spectroscopy using artificial neural networks", Journal of the European Optical Society – Rapid Publications, 3, 08011(1-5), ISSN 1990-2573, (2008).
[25] A. Koujelev, V. Motto-Ros, D. Gratton, and A. Dudelzak, "Laser-induced breakdown spectroscopy as geological tool for field planetary analogue research", Canadian Aeronautics and Space Journal, 55, 2, pp. 97–106, (2009).